Polímeros
ISSN: 1678-5169
Associação Brasileira de Polímeros

Dias, André Rocha Monteiro; Miranda, Beatriz Nogueira Messias de; Cobas-Gomez, Houari; Poço, João Guilherme Rocha; Rubio, Mario Ricardo Gongora; Oliveira, Adriano Marim de

Synthesis and characterization of amphiphilic block copolymers by transesterification for nanoparticle production

Polímeros, vol. 29, no. 2, 2019
Associação Brasileira de Polímeros

DOI: 10.1590/0104-1428.02918

Polímeros
ISSN 1678-5169 (Online)

https://doi.org/10.1590/0104-1428.02918

ORIGINAL ARTICLE

Synthesis and characterization of amphiphilic block copolymers by transesterification for nanoparticle production

André Rocha Monteiro Dias[1], Beatriz Nogueira Messias de Miranda[1], Houari Cobas-Gomez[2], João Guilherme Rocha Poço[3], Mario Ricardo Gongora Rubio[1] and Adriano Marim de Oliveira[1]*

[1]Núcleo de Bionanomanufatura – BIONANO, Instituto de Pesquisas Tecnológicas do Estado de São Paulo – IPT, São Paulo, SP, Brasil

[2]SCINNTECH, São Paulo, SP, Brasil

[3]Departamento de Engenharia Química – DEQ, Centro Universitário da Fundação Educacional Inaciana – FEI, São Bernardo do Campo, SP, Brasil

**amarim@ipt.br*

Abstract

Poly(ε-caprolactone)-block-poly(ethylene glycol)-poly(ε-caprolactone) (PCL-PEG-PCL, triblock) and Poly(ε-caprolactone)-block-(poly(ethylene oxide)−poly(propylene oxide)−poly(ethylene oxide)-poly (ε-caprolactone) (PCL-PEO-PPO-PEO-PCL, pentablock) copolymers were synthesized by transesterification with reduction of PCL molecular mass, enabling fewer reactions, lower temperatures, and eliminating extensive purification steps. Free hydrophilic groups were removed from the samples by selective precipitation, and ^{1}H-NMR, FTIR, GPC and DSC analyses characterized the structure and properties of the resulting copolymers. The detection of remaining hydrophilic groups indicates the formation of the amphiphilic block copolymers (BCPs). Further, we obtained polymeric nanoparticles with monodisperse size distribution profiles by nano-precipitation from both the triblock and the pentablock copolymers using a microfluidic device, resulting 144.6 and 188.9 nm size and 0.093 and 0.102 nm polydispersity index, respectively. The nanoparticle assembly depends on the copolymer composition, and the possibility of nanoparticle assembly corroborates to the block structure of the copolymers, and the success of this synthesis route to obtain BCPs.

Keywords: *copolymers, Pluronic F127®, Poly(ε-caprolactone), Poly(ethylene glycol), transesterification.*

How to cite: Dias, A. R. M., Miranda, B. N. M., Cobas-Gomez, H., Poço, J. G. R., Rubio, M. R. G., & Oliveira, A. M. (2019). Synthesis and characterization of amphiphilic block copolymers by transesterification for nanoparticle production. *Polímeros: Ciência e Tecnologia, 29*(2), e2019027. https://doi.org/10.1590/0104-1428.02918

1. Introduction

Over the past decades, poorly water-soluble compounds have shown their potential as drug candidates[1]. Unfortunately, despite the extensive development and applicability of these hydrophobic therapeutic agents, efficient delivery is often a challenge. Due to their frequently low molecular weight, rapid clearance occurs within the body, and the use of high doses is needed to compensate for its clearance and achieve therapeutic doses. Also, their organ and tissue distribution are often nonspecific, which enhances the probability of its accumulation in healthy tissues, enhancing toxicity and undesirable side effects, obviating the need for delivery alternatives[2].

Among numerous available strategies to achieve trigger-release, the use of block copolymer systems has proven effectiveness[3-5]. Its diversity and versatility meet the need for more continuous therapeutic drug effect, enabling the transport and release of the active agent at specific sites, specific times or after a specific stimulus, increasing efficiency and minimizing side effects[6-8]. Moreover, its mechanical and physicochemical properties, in general, can be changed and improved by simple manipulation of the amphiphilic block and its ratio. Such characteristic together with the production of self-assembled structures, commercial availability, biocompatibility, biodegradability, ease of synthesis and the ability to stabilize hydrophobic compounds that are otherwise insoluble in an aqueous environment make block copolymers an exciting class of materials with countless applications, including medicine. Therefore, the use of block copolymers in controlled drug delivery foments the research of the different amphiphilic copolymers combinations and different synthesis routes.

A mandatory characteristic regarding drug carriers based on block copolymers are the biocompatibility and the biodegradability of the polymeric building blocks. Among amphiphilic copolymers, poly (ethylene glycol) (PEG) and some poloxamers (poly(ethylene oxide)−poly(propylene oxide)−poly(ethylene oxide), PEO−PPO−PEO) such as Pluronic F127® (F127) are known to provide interesting surface

properties to the nanocarrier, are commercially available, biodegradable and are safe for internal use, what make them interesting for scientific and technological purposes[9]. Among the hydrophobic ones, poly (ε-caprolactone) (PCL) holds unique properties such as biodegradation within the body due to hydrolysis of its ester bonds. Moreover, PCL is an important starting point for building advanced polymer architectures[10]. For instance, ε-caprolactone (ε-CL) polymerization can be achieved by direct condensation, and by the use of anionic, cationic and nonionic-nucleophile initiators. However, block copolymers synthesis, in special the ones associated to PCL, often relies on ring-opening polymerization (ROP) routes that frequently depend upon high polymerization temperatures; long polymerization time; and multiple and extensive reaction steps, exemplified ROP reactions are shown in Table 1.

As an alternative, transesterification reaction has been used to obtain polymers with a narrow distribution of molecular weights and functionalized, i.e., with hydroxyl sides (diol polymers). The use of this process enables the production of hydroxyl telechelic polymers that can, for instance, be used to obtain block copolymers or to insert signaling structures. Several studies were conducted to obtain polymers with narrow molecular weight distribution and hydroxyl terminations through trans-esterification for block polymers production[24-28].

A reduction in the use of toxic reagents, reaction time, and steps lead to an increase in efficiency in the synthesis process, not requiring extensive purification steps. Therefore, in this paper, the poly(ε-caprolactone)-block-poly(ethylene glycol)-poly(ε-caprolactone) (PCL-PEG-PCL, triblock) and the poly(ε-caprolactone)-block-(poly(ethylene oxide)−poly(propylene oxide)−poly(ethylene oxide)-poly (ε-caprolactone) (PCL-PEO-PPO-PEO-PCL, pentablock) copolymers are synthesized by transesterification with reduction of PCL molecular weight, in the presence of Pluronic F-127® or PEG. The resulting copolymers were characterized by gel permeation chromatography (GPC), 1H nuclear magnetic resonance (1H NMR), Fourier transform infrared spectroscopy (FTIR), and differential scanning calorimetry (DSC). This procedure represents an easy and low-cost way to obtain block copolymers with a degree of blockiness different from those previously reported[9,29,30].

Additionally, this paper also shows some interesting results of using synthesized block copolymer as building units for active pharmaceutical compounds nanocapsules synthesis by the microfluidic route employing nanoprecipitation strategy. It was used a homemade microfluidic device for nanoprecipitation, which is a development of the nanonization technique used for nanoparticle generation in fields like drug formulation and chemistry, among others[31-37].

2. Materials and Methods

2.1 Materials

Pluronic F-127® (M_{wF127} is 12,600 g·mol^{-1}) was purchased from Viabrasil, polycaprolactone 80,000 g·mol^{-1} (PCL) from Sigma-Aldrich, poly(ethylene glycol) (PEG, M_{wPEG} 6,000 g·mol^{-1}) from Synth, Diadema, Brazil and p-toluene sulfonic acid, PA, from Anidrol for block copolymer synthesis. All used solvents

Table 1. Literature review - ROP reactions.

Functional reactant ending groups	Catalyst	Reaction	Reference
OH	$Sn(Oct)_2$	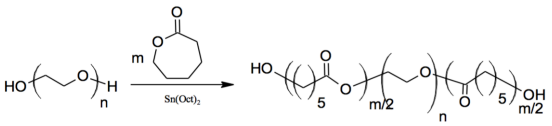	[11-17]
NH_2		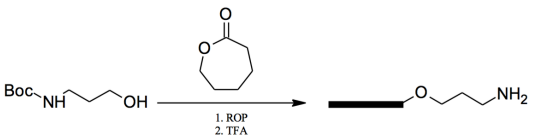	[18]
Epoxy		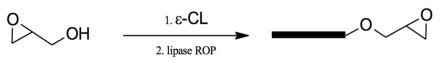	[19]
Br		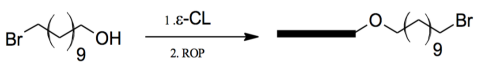	[20]
Triple bond	Ítrium complex	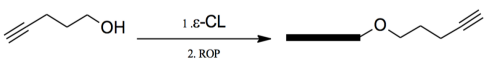	[21]
Sangers solvent		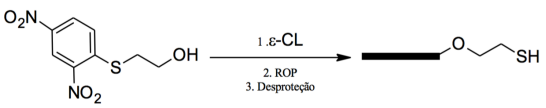	[22]
	$Nd(BH_4)_3(THF)_3$	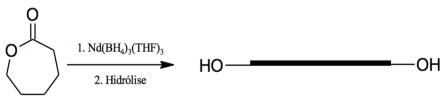	[23]

and salts were from Dinâmica Química Contemporânea Ltda, Diadema, Brazil.

2.2 Synthesis methods of block copolymers

A Dean Stark apparatus setup was used for all reactions. It consists of a 500 mL round bottom flask, reflux condenser, heating mantle with magnetic stirring and thermometer with sodium sulfate as drying material. An adaptation of a literature procedure enabeled the preparation of PCL-F127-PCL and PCL-PEG-PCL[26]. The initial polymers and the catalyst 4-toluenesulfonic acid (p-TSA) were dissolved in 150 mL of toluene. The mixture was kept under reflux at 110 °C. Table 2 shows all specific quantities, together with the reactions times. Reactions C and D were kept stirring for 2 hours before reflux. The solute concentration at the beginning of the reaction was between 25-50 mg·mL^{-1}. After cooling to room temperature, the remaining solvent in the sample was removed using a rotatory evaporator. Then, the content was dissolved in 5 mL of dichloromethane (DCM). The amphiphilic block copolymer was isolated from hydrophilic polymers by selective precipitation with 50 mL of cold ethanol, under magnetic stirring. Finally, the material was dried at 40 °C for 24 hours.

2.3 Purification of block copolymers

The produced amphiphilic block copolymers were recovered by selective precipitation method with cold ethanol as non-solvent for hydrophobic blocks, under magnetic stirring. The material was dried at 40 °C for 24 hours. The block diagram illustrates this procedure, shown in Figure 1.

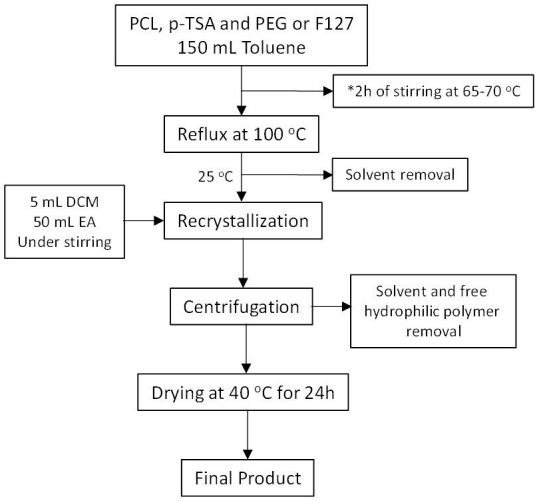

Figure 1. Bock diagram representing the production and purification methods used. *Only for reactions C and D.

2.4 Characterization of block copolymers

2.4.1 Determination of molecular weight by Gel Permeation Chromatography (GPC)

Viscotek TDAmax equipment, 2X Viscogel column and refractive index detector were used for GPC analysis, and a method was validated according to a standard procedure based on the comparison of chromatographic profiles of mixtures of different molecular weight polystyrene (PS) standards. Briefly, tetrahydrofuran (THF) at 0.5 mL·min^{-1} flow rate was used as the chromatography eluent and 35 °C as the column's and detector's temperature. The sample was dissolved in THF (10 mg·mL^{-1}) and 100 µL of this solution was injected into the chromatography column for conducting the GPC analysis.

2.4.2 Hydrogen Nuclear Magnetic Resonance Analysis (1H NMR)

Agilent 400 MR spectrometer conducted the 1H NMR measurements at a frequency of 400 MHz at 25 °C. Approximately 7 mg of each sample was dissolved in 600 µL of deuterochloroform ($CDCl_3$), containing 0.05% of tetramethylsilane (TMS) to reference the chemical shift.

The values of the molar masses were estimated as follows: the value of 195 protons was attributed to the characteristic signal of propylene glycol methyl in 1.13 ppm of F127, from the molar mass value provided by the manufacturer. Integrations of other signs provided the other amounts of protons. The molar mass of the block copolymer was obtained by the sum of the molar mass F127 (12,600 g·mol^{-1}) plus the mass of PCL incorporated, according to Equation 1. The PCL mole number was obtained by Equation 2.

$$M(cba) = \frac{12.600g}{mol} + \frac{n(cl) * 114g}{mol} \quad (1)$$

$$n(cl) = 195 * \frac{\int 4\,ppm}{2} \quad (2)$$

Where:

M (cba) = molar mass of amphiphilic block copolymer (g.mol^{-1}).

n (cl) = number of mols of caprolactone (mol).

2.4.3 Attenuated total reflectance with Fourier transform infrared (ATR - FTIR)

The IR spectra were obtained for solid samples using a Nicolet 6700 FT-IR spectrometer fitted with ATR, in the range of 4000 to 700 cm^{-1} and 128 accumulations. The Smart OMNI software was used for data processing.

2.4.4 Differential Scanning Calorimetry Analysis (DSC)

The samples were prepared using a sealed aluminum pan and analyzed by Shimadzu DSC-60. Three temperature ramps were done as follows: -80 °C to 120 °C; 120 °C to

Table 2. Compositions and reaction times of the PCL/F127/PCL pentablock and PCL/PEG/PCL triblock copolymers synthesis.

Reaction	F127/PCL (m/m)	PEG/PCL (m/m)	p-TSA (wt. %)	Reaction time (h)
A	-	0.63	2.5	18
B	0.63	–	1.5	18
C	2	–	7	4
D	–	2	7	4

-80 °C; and -80 °C to 120 °C; all at 10 °C·min^{-1} heating and cooling rates and with 50 mL·min^{-1} nitrogen gas flow.

2.5 Block copolymer nanocapsule synthesis and characterization

2.5.1 Microfluidic device

For nanocapsule synthesis, in-flow nanoprecipitation technique was used. In this technique, block copolymers and active pharmaceutical compound were dissolved using acetone to obtain an organic solution. This solution is placed in contact with an antisolvent flow inside the microfluidic device. High material concentration regions are created due to the solvent diffusion from the organic phase into the antisolvent flow. At these regions the material is no longer soluble in the solvent - antisolvent mixture, increasing its concentration. When a material concentration exceeds a critical level, spontaneous nucleation takes place, generating nanoparticles[38, 39].

For implementing the nanoprecipitation strategy using microfluidics techniques, a 3D flow focalization homemade LTCC (Low Temperature Co-fired Ceramic) microfluidic device was fabricated, Figure 2a. The device consists in an organic phase input, dissolved material, DM, (Hydraulic Diameter DH = 214.6 µm), the anti-solvent (AS) inputs and the nanoprecipitation channel (NPC) (DH = 772 µm and length 6.5 mm). The DM and NPC channels are centered. The four AS inputs have an input angle of 45º to the NPC direction. Device inputs geometry makes possible the 3D flow focalization which highly improves the nanoprecipitation process due to a better solvent diffusion process from the dissolved material flow stream to the surrounding antisolvent flow[39,41].

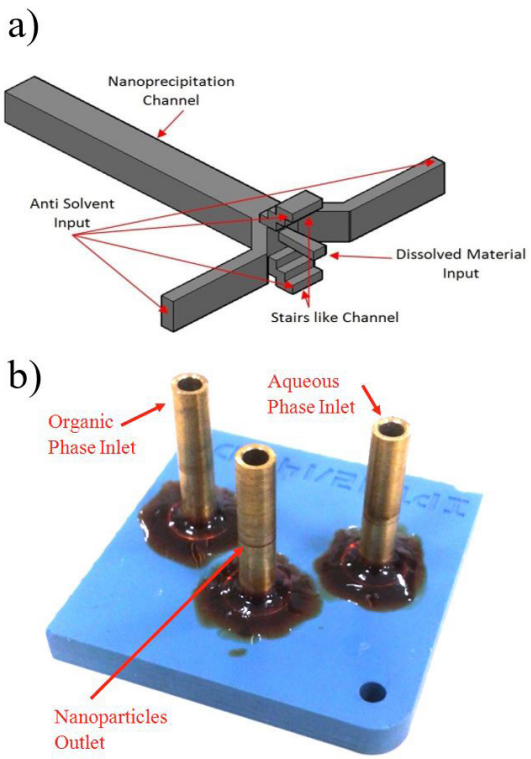

Figure 2. 3D Hydrodynamic focalization microfluidic device. a) Micro channels geometry; b) Manufactured microfluidic device. Anti-solvent = Organic Phase; Dissolved Material = Aqueous Phase. Adapted from Cobas-Gomez[39] and Cobas-Gomez et al.[40].

Microfluidic device fabrication employed the typical LTCC process[40]. DuPont green LTCC ceramic tapes 951P2 and 951PX were used. Layers were fabricated using a prototyping machine equipped with an ultraviolet laser (355 nm wavelength), model LPKF Protolaser U3 (LPKF Laser & Electronics AG). One step thermo-compression lamination process was performed by means of a uniaxial laminator with a pressure of 11.8 MPa at 70 °C (hydraulic press machine, model MA098/A30, Marconi). Previous to the lamination process, the aligned sheets were baked at 60 °C for 20 min. For sintering we used a muffle furnace (EDG Equipment, model EDG10P-S), in a two-stage profile: first, heating the device at 450 °C for 30 min. and in sequence, sintering at 850 °C per 30 min.

The input and output brass fluidic interconnection tubes were glued to the ceramics using a high-temperature epoxy (EPO-TEK 353ND). For the gluing process, a hot plate at 150 °C for 2 min was used. The fabricated 3D flow focalization microfluidic device is showed in Figure 2b).

2.5.2 Sample preparation

Organic phase fluid dissolved material was prepared from 1 g of synthesized pentablock PCL-F127-PCL copolymers and 100 mg of Hydrocortisone Acetate and mixed in 20 mL of Acetone (Sigma Aldrich) until complete dissolution. As Antisolvent (AS) fluid material we used 100 mL of purified DI water (Aqueous phase). A Milli-Q system (Millipore Corporation, USA) was employed to obtain the purified water.

For pumping the DM and AS into the microfluidic device at the desired flow rate (Q_{DM} and Q_{AS}, respectively) two syringe pumps (PHD 4400, Harvard Apparatus) were used.

2.5.3 Dynamic Light Scattering (DLS)

DLS analyses were carried out using a laser particle analyzer (Zetasizer Nano ZS, Malvern Instruments) using the manufacturer's software as the calculation method, in water. DLS measurements were based on 3 repetitions of 70 accumulation times. Samples were analyzed at 25 °C with a scattering angle of 90° and at 633 nm, based on a dispersant refractive index (RI) of 1.33, a viscosity of 0.89 and a dielectric constant of 78.3.

3. Results and Discussions

3.1 Synthesis and Characterization of PCL/F127/PCL and PCL/PEG/PCL block Copolymers

PCL/PEG/PCL triblock (reactions A and D) and PCL/F127/PCL pentablock (reactions B and C) copolymers were successfully synthesized by transesterification (Table 2). ^{1}H-NMR spectrums were recorded to confirm the structure of the copolymers. In the spectra of the triblock produced by reactions A and D, shown in Figures 3b and c, the peaks at 3.64 ppm were attributed to the ethylene protons of the PEG ethylene glycol units

(a, b). Peaks of ethylene glycol units were also found in the spectra of pentablock PCL/F127/PCL produced by reactions B and C, and attributed to the F127 units (a, b), shown in Figures 4b and c. Due to the high molecular weight of the analyzed copolymers, only a weak ^{1}H-NMR signal at 4.23 ppm is seen from terminal ethylene units of PEG, but it was still characterized for all samples, as shown in Supplementary Material S1-S4. In Figures 4b and c, the very weak peak at 1.14 ppm was identified as the methyl protons of the F127 unit (c), and was not identified in the PEG copolymer due to the absence of methyl protons in the PEG copolymer structure, shown in Figure 3a. Peaks at 1.38, 1.65, 2.31, and 4.06 ppm were assigned to the methylene protons in PCL units (identified as f, e, d, g, respectively), and therefore present in all copolymer products, both tri and pentablocks due to the existence of PEG units, which is very similar to the literature reported spectrum. In particular, the weak 4.06 ppm peak correlates to the methylene protons of a PEG and F127 end units that are connected with PCL blocks[42]. It is important to remind that free F127 and PEG groups were isolated from free PCL and freshly prepared block copolymers by selective precipitation using ethanol. Therefore, we can assume that only PCL-linked hydrophilic blocks are present

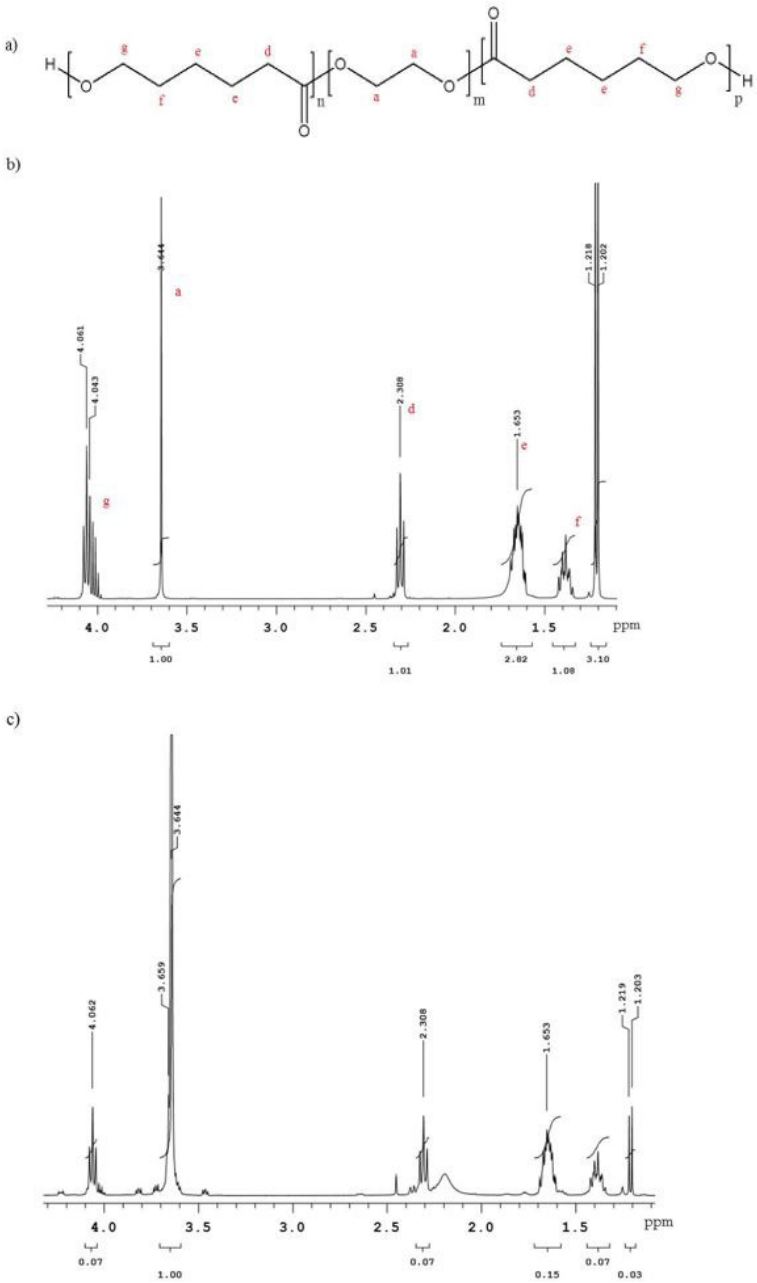

Figure 3. BCP formula (a) and ^{1}H-NMR spectrum of PCL/PEG/PCL triblock copolymer, reactions A (b) and D (c), respectively.

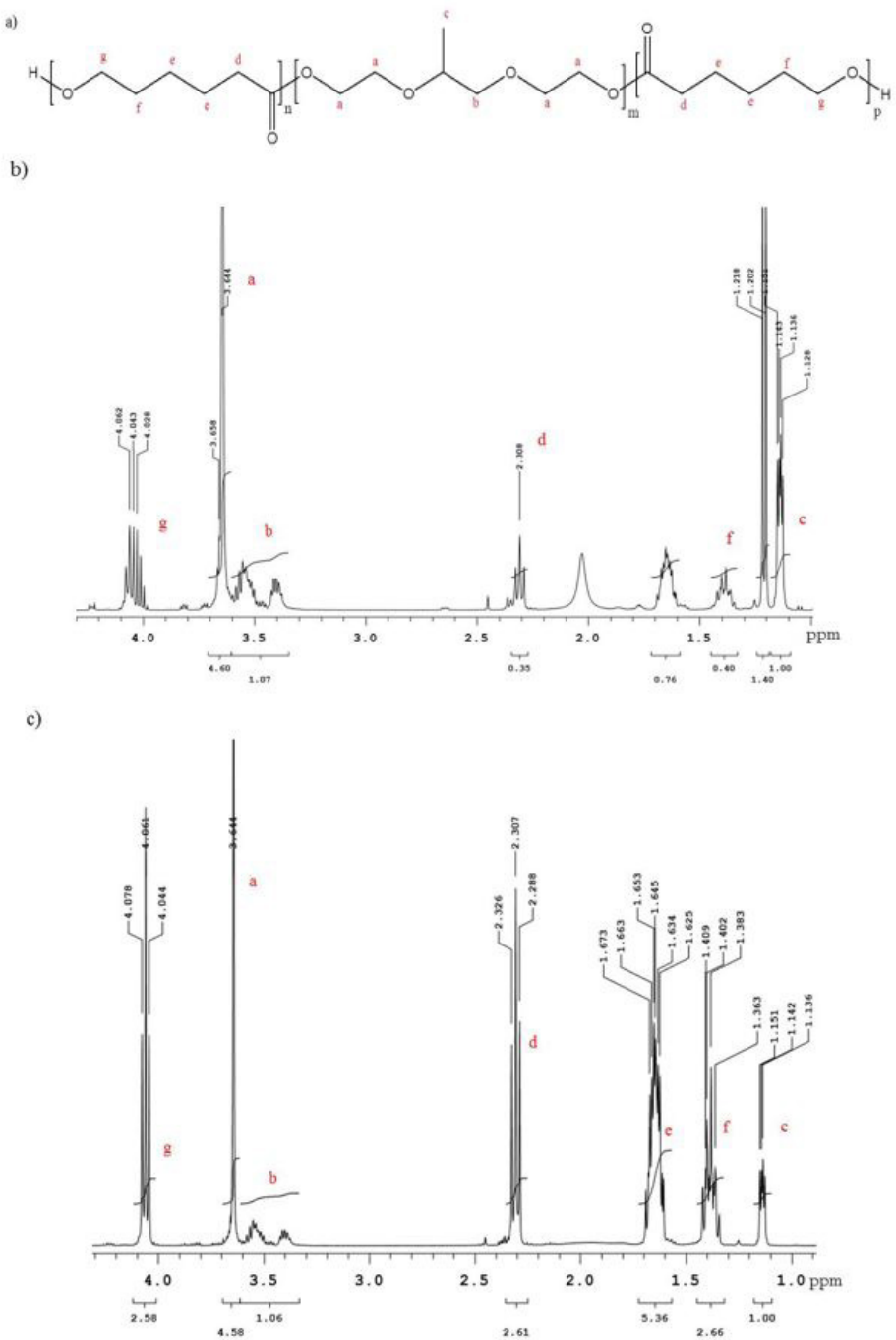

Figure 4. BCP formula (a) and ^{1}H-NMR spectrum of pentablock PCL/F127/PCL pentablock copolymer, reactions B (b) and C (c), respectively.

in the precipitate. This assumption enables the M_{wNMR} of the PCL/F127/PCL copolymers and the PEG/PCL block ratios calculation by comparing the PCL 4.06 ppm and the PEG or F127 3.64 ppm integrated peaks[29, 43].

From GPC traces (shown in Figure 5), shifts in profile and retention volumes are seen. The chromatogram of the physical mixture of PCL and F127 is shown in Figure 5a, and the peak at a retention volume of 25.19 mL was attributed to PCL, due to its higher molecular weight, while the higher retention volume signal, of 28.17 mL, was attributed to F127. The profile of this chromatogram can be compared to the ones on Figures 5c and d that shows the GPC curves of pentablock copolymers produced in reactions B and C, respectively. Although the product's curve is not unimodal, a shift in profile and retention volumes is observed for both cases. Considering that most of the non-reacted hydrophilic

blocks were removed from the copolymer sample by selective precipitation, it is presumable that only the ones linked to PCL are left. Moreover, the peak shift to the right of the chromatogram seen when comparing Figures 4a physical mixture and c) or d) pentablock copolymer samples can be explained by a decrease in the PCL molar masses, which leads to its linkage to hydrophilic blocks. The same can be extended to the triblock copolymer produced in reaction D, shown in Figure 5e, and using PEG instead of F127 (which chromatogram is shown in Figure 5b). Consistency in the data can be observed when compared to NMR and FTIR results shown in Table 3, in special for lower molar masses. (Chromatographic profiles of mixtures of different molecular weight polystyrene (PS) standards and MW curve are shown in Supplementary Material S5-S6).

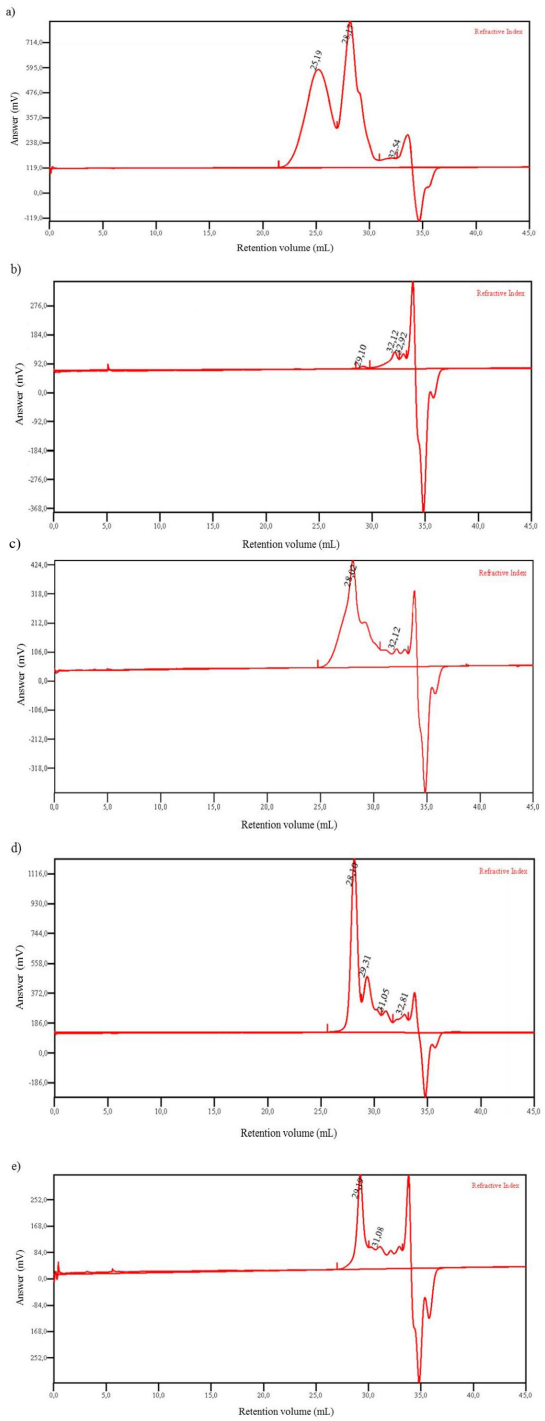

Figure 5. GPC curves of (a) physical mixture of PCL and F127; (b) pure PEG; the block copolymer product after the trans esterification reactions (c) B; (d) C; and (e) D.

The Figures 6a and b show FTIR spectra for reactions A and B, tri and pentablock copolymers. These results were interpreted considering the polyester and polyether characteristic signals, which are attributed to 1,724 cm^{-1} and 1,108 cm^{-1}, respectively. The absorption band at 1,724 cm^{-1} is attributed to the characteristic polyester C=O stretching vibrations of the ester carbonyl group from PCL, while 1,108 cm^{-1} can be attributed to C−O−C stretching vibrations of the repeated $-OCH_2CH_2$ groups of PEG (or F127). Once the reaction products were purified by selective precipitation using ethanol, free PEG and F127 were removed from the sample, and still, the presence of both groups in the sample was confirmed by FTIR, indicating block copolymer formation.

Curves that relate the peaks 1,108 cm^{-1} and 1,724 cm^{-1} ratio value (I_{1108} / I_{1724} ratio) with its molecular weights were obtained using the specific molar mass values previously acquired from ^{1}H-NMR spectra and GPC chromatograms. Different curves were prepared for samples using F127 and PEG as the hydrophilic block (pure PCL and F127 spectrum as well as curves for PCL/PEG/PCL and PCL/F127/PCL are shown in Supplementary Material S7-S9). This way, according to the obtained I_{1108} / I_{1724} ratio, we could presume the M_{FTIR} for each sample, as shown in Table 3.

The results obtained by FTIR-ATR are consistent with those obtained by NMR and GPC, therefore, indicating the formation of the block copolymers products.

Thermal analyses were performed on the PCL and F127 reagents and compared to the results obtained for the sample from Reaction B (PCL/F127/PCL). Both the melting temperature and the crystallinity degree (analyzed by the enthalpy of fusion) of the polymer sample displayed a decrease when compared to individual components. This can be explained by the PCL´s molar mass reduction. The obtained melting point and enthalpy of fusion are presented in Table 4 (graphs are shown in Supplementary Information S11-S13).

Table 3. Molecular weights (g mol^{-1}) of the PCL/PEG/PCL triblock (reactions A and D) and PCL/F127/PCL (reactions C and D) pentablock copolymers.

Sample	M_{FTIR} [a]	M_{NMR} [b]	M_{GPC} [c]
A	25.052	36.923	-
B	30.679	30.717	17.252
C	16.683	17.046	16.341
D	8.602	8.186	7.916

[a] Calculated according to the I_{1108} / I_{1724} ratio of the FTIR-ATR peaks. [b] Number-average molecular weight calculated from ^{1}H NMR Spectrum. [c] Number-average molecular weight measured by GPC (calibrated with polystyrene standards).

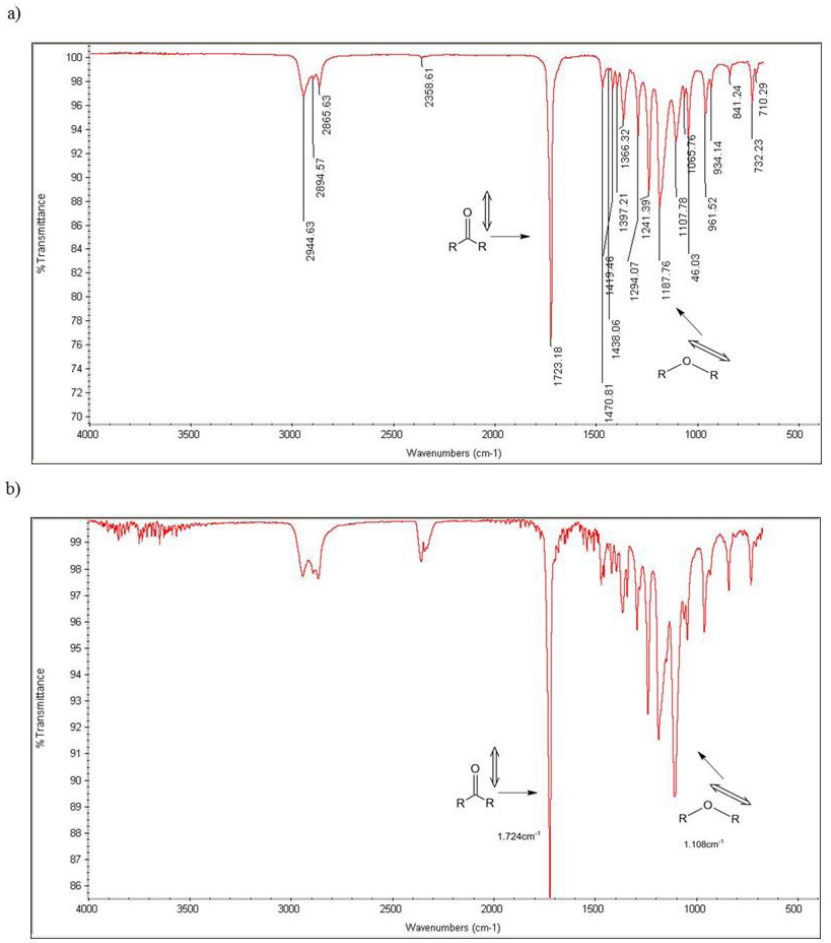

Figure 6. Sample FTIR spectrum of PCL/PEG/PCL triblock copolymer from reaction A and PCL/F127/PCL pentablock copolymer from reaction B. Marked peaks are attributed to polyester and polyether characteristic signals.

Table 4. Table of results from DSC curves of PCL, F127 and amphiphilic block copolymer product from Reaction B.

Material	Melting Point (°C)	Enthalpy of fusion ($J \cdot g^{-1}$)
PCL	59.05	-54.33
F127	58.06	-99.84
Reaction B	44.76	-8.54
	53.64	-31.94

3.2 Influence of the hydrophilic block on copolymer formation

The influence of the hydrophilic block´s size on the copolymer formation was analyzed. As a matter of comparison, the same procedure used for producing a pentabock copolymer (Reaction C, containing F127) was used for producing a triblock copolymer (Reaction D), containing only PEG as a hydrophilic block, as shown in Table 3. The Pluronic® F127 is a poloxamer that has 2 polyethylene oxide, PEG, groups on the outside and polypropylene oxide, PPO, as the inner block. The same mass ratio F127/PCL and PEG/PCL was used, remembering that M_{wF127} is 12,600 $g \cdot mol^{-1}$ and M_{wPEG} is 6,000 $g \cdot mol^{-1}$. ^{1}H-NMR, GPC, and FTIR analysis were promoted (as shown in Figures 3-5 and Supplementary Material S14-S15), all the FTIR and ^{1}H-NMR results indicated that the PCL-PEG-PCL copolymers were formed successfully, and the amount of PCL incorporated could be calculated, resulting 4,446 $g \cdot mol^{-1}$ e 2,166 $g \cdot mol^{-1}$ for reactions C and D, respectively. According to this result, there is a direct relationship between each hydrophilic block M_w and the amount of incorporated PCL, indicating similar reactivity among the terminal hydroxyl groups.

3.3 Synthesis of amphiphilic block copolymers particles using microfluidics

Triblock copolymer particles were successfully obtained using a microfluidic device as described before. A value of 144.6 nm with a polydispersity index of 0.093 was obtained for block copolymer from Reaction A, indicating the formation of particles with nanometric dimensions and low polydispersity. The occurrence of nanoparticle corroborates with the PEG – PCL biding since the simple physical mixing of these materials would not permit the particle formation.

Table 5. Table of results from block copolymer capsules synthesis using the microfluidic device. Adapted from Cobas-Gomez et al.,[40] The total flow rate (Q_T) is defined as the sum of Q_{DM} and Q_{AS}, and the flow rate ratio (R_Q) defined as the ratio between Q_{AS} and Q_{DM}.

R_Q	Q_T (aqueous + organic flow rate; mL·min^{-1})	Particle size (nm)	PDI
1.3	1	459.1	0.235
10	1	287.8	0.228
1.3	7.5	355.5	0.206
10	7.5	188.9	0.102
6.26	4.64	233.4	0.188

$Q_T = Q_{DM} + Q_{AS}$. $R_Q = Q_{AS}/Q_{DM}$.

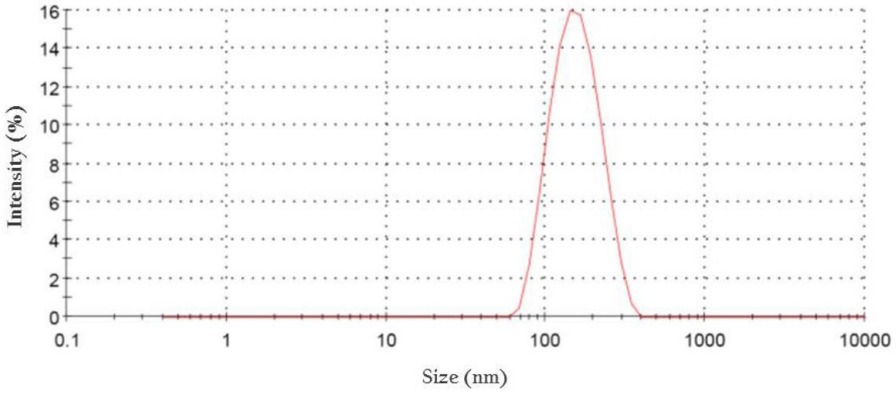

Figure 7. Particle size distribution of PCL/PEG/PCL nanoparticles produced with Sample A and microfluidic device, using Flow rate ratio, $R_Q = 10$ and Total flow rate, $Q_T = 7.5$ mL·min^{-1}.

The pentablock copolymer obtained by Reaction B was used as the polymeric carrier for a pharmaceutical compound. The experiment variables were the total flow rate (Q_T) defined as the sum of Q_{DM} and Q_{AS}, and the flow rate ratio (R_Q) defined as the ratio between Q_{AS} and Q_{DM}. A factorial experiment planning approach was used to set the variables values. The experiment parameters and results are presented in Table 5. Results showed sub-micron and nanocapsules with sizes ranging from 459.1 nm to 188.9 nm. The polydispersity index remains lower than 0.235 which implies a narrow particle size distribution. A monodisperse particle size distribution profile (Size = 188.9 nm and PDI = 0.102) was observed for the sample obtained with experimental parameters $R_Q = 10$ and $Q_T = 7.5$ mL·min^{-1}, and the distribution performed with the previously mentioned sample is shown in Figure 7.

Therefore, the use of both triblock and pentablock copolymers produced by transesterification reactions enabled nanoparticle production by the use of a microfluidic preparation.

4. Conclusions

This study demonstrates the use of transesterification with polyester molecular weight reduction as a versatile and straightforward approach for obtaining amphiphilic block copolymers. Concerning the FTIR-ATR, ^{1}H NMR, and GPC results and assuming that the majority of free hydrophilic groups were removed from the analyzed sample by selective precipitation with ethanol, it is clear that polyester and polyether groups are presented in the product indicating the formation of the amphiphilic block copolymers. The results obtained for the molecular weights are consistent among the different techniques and also close to the theoretical values. For the thermal analysis results, there was a decrease in both melting temperature and enthalpy of fusion. Since these parameters are related to the crystallinity and, consequently, the samples' molecular weight, these decreases indicate the PCL molar mass reduction, an increase in biodegradability and proves the successful synthesis of amphiphilic block copolymers. Moreover, polymeric nanoparticles with sizes ranging from 459.1 nm down to 188.9 nm were successfully produced with a narrow polydispersity (0.235 down to 0.102) by nano-precipitation using a microfluidic device. The fact that particles have been produced with the product of the transesterification reactions already proves the synthesis of amphiphilic block copolymers since non-linked blocks would not enable particle production. We believe that this production technique is of extreme value for the reduction in the use of toxic reagents, and the simplification of block copolymers synthesis. Finally, the possibility of using a wide molecular weight range of polyesters, avoiding cyclization steps and molecular weight reduction, together with the advancing of nano theraphy will provide further knowledge and possible new carriers for disease treatment and diagnostic.

5. Acknowledgments

We acknowledge the Institute for Technological Research, IPT, and the Institute for Technological Research Foundation, FIPT, for infrastructure and A.R.M.D. and B.N.M.M. funds; the Centro Universitário da FEI for the support; and the Coordination for the Improvement of Higher Level Personnel, CAPES, for the support.

6. References

1. Lipinski, C. A. (2002). Poor aqueous solubility: an industry wide problem in drug discovery. *American Pharmaceutical Review*, *2*(3), 82-85.
2. Lammers, T., Kiessling, F., Hennink, W. E., & Storm, G. (2011). Drug targeting to tumors: principles, pitfalls and (pre-) clinical progress. *Journal of Controlled Release*, *161*(2), 175-187. http://dx.doi.org/10.1016/j.jconrel.2011.09.063. PMid:21945285.
3. Kabanov, A. V., Batrakova, E. V., & Alakhov, V. Y. (2002). Pluronic® block copolymers for overcoming drug resistance in cancer. *Advanced Drug Delivery Reviews*, *54*(5), 759-779. http://dx.doi.org/10.1016/S0169-409X(02)00047-9. PMid:12204601.
4. Letchford, K., & Burt, H. (2007). A review of the formation and classification of amphiphilic block copolymer nanoparticulate structures: micelles, nanospheres, nanocapsules and polymersomes. *European Journal of Pharmaceutics and Biopharmaceutics*, *65*(3), 259-269. http://dx.doi.org/10.1016/j.ejpb.2006.11.009. PMid:17196803.
5. Smart, T., Lomas, H., Massignani, M., Flores-Merino, M. V., Perez, L. R., & Battaglia, G. (2008). Block copolymer nanostructures. *Nano Today*, *3*(3-4), 38-46. http://dx.doi.org/10.1016/S1748-0132(08)70043-4.
6. Bae, S. J., Suh, J. M., Sohn, Y. S., Bae, Y. H., Kim, S. W., & Jeong, B. (2005). Thermogelling Poly(caprolactone-b-ethylene glycol-b-caprolactone) Aqueous Solutions. *Macromolecules*, *38*(12), 5260-5265. http://dx.doi.org/10.1021/ma050489m.
7. Lucke, A., Te, K., Schnell, E., Schmeer, G., & Go, A. (2000). Biodegradable poly(D,L-lactic acid)-poly(ethylene glycol)-monomethyl ether diblock copolymers: Structures and ether diblock copolymers: structures and surface properties relevant to their use as biomaterials. *Biomaterials*, *21*(23), 2361-2370. http://dx.doi.org/10.1016/S0142-9612(00)00103-4. PMid:11055283.
8. Vila, A., Sanchez, A., Tobıo, M., Calvo, P., & Alonso, M. J. (2002). Design of biodegradable particles for protein delivery. *Journal of Controlled Release*, *78*(1-3), 15-24. http://dx.doi.org/10.1016/S0168-3659(01)00486-2. PMid:11772445.
9. Meier, M. A. R., Aerts, S. N. H., Staal, B. B. P., Rasa, M., & Schubert, U. S. (2005). PEO-b-PCL block copolymers: Synthesis, detailed characterization, and selected micellar drug encapsulation behavior. *Macromolecular Rapid Communications*, *26*(24), 1918-1924. http://dx.doi.org/10.1002/marc.200500591.
10. Sisson, A. L., Ekinci, D., & Lendlein, A. (2013). The contemporary role of ε -caprolactone chemistry to create advanced polymer architectures. *Polymer*, *54*(17), 4333-4350. http://dx.doi.org/10.1016/j.polymer.2013.04.045.
11. Báez, J. E., Marcos-Fernández, Á., Lebrón-Aguilar, R., & Martínez-Richa, A. (2006). A novel route to α,ω-telechelic poly(ε-caprolactone) diols, precursors of biodegradable polyurethanes, using catalysis by decamolybdate anion. *Polymer*, *47*(26), 8420-8429. http://dx.doi.org/10.1016/j.polymer.2006.10.023.
12. Cho, H. K., Cho, K. S., Cho, J. H., Choi, S. W., Kim, J. H., & Cheong, I. W. (2008). Synthesis and characterization of PEO-PCL-PEO triblock copolymers: Effects of the PCL chain length on the physical property of W1/O/W2 multiple emulsions. *Colloids and Surfaces. B, Biointerfaces*, *65*(1), 61-68. http://dx.doi.org/10.1016/j.colsurfb.2008.02.017. PMid:18400473.
13. Gong, C. Y., Wu, Q. J., Dong, P. W., Shi, S., Fu, S. Z., Guo, G., Hu, H. Z., Zhao, X., Wei, Y. Q., & Qian, Z. Y (2009). Acute toxicity evaluation of biodegradable in situ gel-forming controlled drug delivery system based on thermosensitive PEG-PCL-PEG hydrogel. *Journal of Biomedical Materials Research. Part B, Applied Biomaterials*, *91*(1), 26-36. http://dx.doi.org/10.1002/jbm.b.31370. PMid:19365823.
14. Hu, Y., Xie, J., Tong, Y. W., & Wang, C. H. (2007). Effect of PEG conformation and particle size on the cellular uptake efficiency of nanoparticles with the HepG2 cells. *Journal of Controlled Release*, *118*(1), 7-17. http://dx.doi.org/10.1016/j.jconrel.2006.11.028. PMid:17241684.
15. Huang, Y., Gao, H., Gou, M., Ye, H., Liu, Y., Gao, Y., Peng, F., Qian, Z., Cen, X., & Zhao, Y. (2010). Acute toxicity and genotoxicity studies on poly(ε-caprolactone)-poly(ethylene glycol)-poly(ε-caprolactone) nanomaterials. *Mutation Research/Genetic Toxicology and Environmental Mutagenesis*, *696*(2), 101-106. http://dx.doi.org/10.1016/j.mrgentox.2009.12.016. PMid:20060489.
16. Lu, F., Lei, L., Shen, Y. Y., Hou, J. W., Chen, W. L., Li, Y. G., & Guo, S. R. (2011). Effects of amphiphilic PCL-PEG-PCL copolymer addition on 5-fluorouracil release from biodegradable PCL films for stent application. *International Journal of Pharmaceutics*, *419*(1-2), 77-84. http://dx.doi.org/10.1016/j.ijpharm.2011.07.020. PMid:21803141.
17. Ahmed, A., Wang, H., Yu, H., Zhou, Z. Y., Ding, Y., & Hu, Y. (2015). Surface engineered cyclodextrin embedded polymeric nanoparticles through host-guest interaction used for drug delivery. *Chemical Engineering Science*, *125*, 121-128. http://dx.doi.org/10.1016/j.ces.2014.07.045.
18. Le Hellaye, M., Fortin, N., Guilloteau, J., Soum, A., Lecommandoux, S., & Guillaume, S. M. (2008). Biodegradable Polycarbonate- b -polypeptide and Polyester- b -polypeptide Block Copolymers: Synthesis and Nanoparticle Formation Towards Biomaterials. *Biomacromolecules*, *9*(7), 1924-1933. http://dx.doi.org/10.1021/bm8001792. PMid:18529076.
19. Chen, C., Ke, J., Zhou, X. E., Yi, W., Brunzelle, J. S., Li, J., Yong, E. L., Xu, H. E., & Melcher, K. (2013). Structural basis for molecular recognition of folic acid by folate receptors. *Nature*, *500*(7463), 486-489. http://dx.doi.org/10.1038/nature12327. PMid:23851396.
20. Gilson, P. R., Nebl, T., Vukcevic, D., Moritz, R. L., Sargeant, T., Speed, T. P., Schofield, L., & Crabb, B. S. (2006). Identification and stoichiometry of glycosylphosphatidylinositol-anchored membrane proteins of the human malaria parasite Plasmodium falciparum. *Molecular & cellular proteomics*, *5*(7), 1286-1299. http://dx.doi.org/10.1074/mcp.M600035-MCP200. PMid:16603573.
21. Matsumura, S., Hlil, A. R., Lepiller, C., Gaudet, J., Guay, D., Shi, Z., Holdcroft, S., Hay, A. S. (2008). Ionomers for proton exchange membrane fuel cells with sulfonic acid groups on the end-groups: Novel branched poly(ether-ketone)s. *Macromolecules*, *49*(1), 511-512.
22. Carrot, G., Hilborn, J. G., Trollsås, M., & Hedrick, J. L. (1999). Two general methods for the synthesis of thiol-functional polycaprolactones. *Macromolecules*, *32*(16), 5264-5269. http://dx.doi.org/10.1021/ma990198b.
23. Guillaume, S. M., Schappacher, M., & Soum, A. (2003). Polymerization of ε-Caprolactone initiated by Nd(BH4)3(THF)3: Synthesis of hydroxytelechelic poly(ε-caprolactone). *Macromolecules*, *36*(1), 54-60. http://dx.doi.org/10.1021/ma020993g.
24. Deng, X. M., & Hao, J. Y. (2001). Synthesis and characterization of poly(3-hydroxybutyrate) macromer of bacterial origin.

European Polymer Journal, *37*(1), 211-214. http://dx.doi.org/10.1016/S0014-3057(00)00090-2.

25. Špitalský, Z., Lacík, I., Lathová, E., Janigová, I., & Chodák, I. (2006). Controlled degradation of polyhydroxybutyrate via alcoholysis with ethylene glycol or glycerol. *Polymer Degradation & Stability*, *91*(4), 856-861. http://dx.doi.org/10.1016/j.polymdegradstab.2005.06.019.
26. Impallomeni, G., Giuffrida, M., Barbuzzi, T., Musumarra, G., & Ballistreri, A. (2002). Acid catalyzed transesterification as a route to poly(3-hydroxybutyrate-co-ε-caprolactone) copolymers from their homopolymers. *Biomacromolecules*, *3*(4), 835-840. http://dx.doi.org/10.1021/bm025525t. PMid:12099830.
27. Impallomeni, G., Carnemolla, G. M., Puzzo, G., Ballistreri, A., Martino, L., & Scandola, M. (2013). Characterization of biodegradable poly(3-hydroxybutyrate-co- butyleneadipate) copolymers obtained from their homopolymers by microwave-assisted transesterification. *Polymer*, *54*(1), 65-74. http://dx.doi.org/10.1016/j.polymer.2012.11.030.
28. Montoro, S. R., Shigue, C. Y., Sordi, M. L. T., Santos, A. M., & Ré, M. I. (2010). Estudo cinético da redução da massa molar do poli(3-hidroxibutirato-co-3-hidroxivalerato) (PHBHV). *Polímeros: Ciência e Tecnologia*, *20*(1), 19-24. http://dx.doi.org/10.1590/S0104-14282010005000005.
29. Zhou, S., Deng, X., & Yang, H. (2003). Biodegradable poly(ε-caprolactone)-poly(ethylene glycol) block copolymers: Characterization and their use as drug carriers for a controlled delivery system. *Biomaterials*, *24*(20), 3563-3570. http://dx.doi.org/10.1016/S0142-9612(03)00207-2. PMid:12809785.
30. Zhou, Q., Zhang, Z., Chen, T., Guo, X., & Zhou, S. (2011). Preparation and characterization of thermosensitive pluronic F127-b-poly(e{open}-caprolactone) mixed micelles. *Colloids and Surfaces. B, Biointerfaces*, *86*(1), 45-57. http://dx.doi.org/10.1016/j.colsurfb.2011.03.013. PMid:21489759.
31. Stainmesse, S., Orecchioni, A. M., Nakache, E., Puisieux, F., & Fessi, H. (1995). Formation and stabilization of a biodegradable polymeric colloidal suspension of nanoparticles. *Colloid & Polymer Science*, *273*(5), 505-511. http://dx.doi.org/10.1007/BF00656896.
32. Chaudhuri, R. G., & Paria, S. (2012). Core/Shell Nanoparticles: classes, properties, synthesis mechanisms, characterization, and applications. *Chemical Reviews*, *112*(4), 2373-2433. http://dx.doi.org/10.1021/cr100449n.
33. Ezhilarasi, P. N., Karthik, P., Chhanwal, N., & Anandharamakrishnan, C. (2013). Nanoencapsulation techniques for food bioactive components: a review. *Food and Bioprocess Technology*, *6*(3), 628-647. http://dx.doi.org/10.1007/s11947-012-0944-0.
34. Chen, H., Khemtong, C., Yang, X., Chang, X., & Gao, J. (2011). Nanonization strategies for poorly water-soluble drugs. *Drug Discovery Today*, *16*(7-8), 354-360. http://dx.doi.org/10.1016/j.drudis.2010.02.009. PMid:20206289.
35. Chan, H. K., & Kwok, P. C. L. (2011). Production methods for nanodrug particles using the bottom-up approach. *Advanced Drug Delivery Reviews*, *63*(6), 406-416. http://dx.doi.org/10.1016/j.addr.2011.03.011. PMid:21457742.
36. Nagavarma, B. V. N., Yadav, H. K. S., Ayaz, A., Vasudha, L. S., & Shivakumar, H. G. (2012). Different techniques for preparation of polymeric nanoparticles: a review. *Journal of Pharmaceutical and Clinical Research*, *5*, 16-23.
37. Schubert, S. Jr, Delaney, J. T. Jr, & Schubert, U. S. (2011). Nanoprecipitation and nanoformulation of polymers: From history to powerful possibilities beyond poly(lactic acid). *Soft Matter*, *7*(5), 1581-1888. http://dx.doi.org/10.1039/C0SM00862A.
38. LaMer, V. K., & Dinegar, R. H. (1950). Theory, production and mechanism of formation of monodispersed hydrosols. *Journal of the American Chemical Society*, *72*(11), 4847-4854. http://dx.doi.org/10.1021/ja01167a001.
39. Cobas-Gomez, H., Gongora-Rubio, M. R., Agio, B. O., Novais Schianti, J., Kimura, V. T., Marim de Oliveira, A., Ramos, L. W. S. L. & Seabra, A. C. (2015). 3D Focalization microfluidic device built with LTCC technology for nanoparticle generation using nanoprecipitation route. *Journal of Ceramic Science and Technology*, *6*(4), 329-338. http://dx.doi.org/10.4416/JCST2015-00062
40. Gongora-Rubio, M. R., Espinoza-Vallejos, P., Sola-Laguna, L., & Santiago-Avilés, J. J. (2001). Overview of low temperature co-Fired ceramics tape technology for meso-system technology (MsST). *Sensors and Actuators. A, Physical*, *89*(3), 222-241. http://dx.doi.org/10.1016/S0924-4247(00)00554-9.
41. Cobas-Gomez, H. (2016). *Sistemas microfluídicos cerâmicos para miniaturização de processos químicos aplicados à fabricação de nanopartículas* (Master's thesis). Universidade de São Paulo, São Paulo.
42. Saghebasl, S., Davaran, S., Rahbarghazi, R., Montaseri, A., Salehi, R., & Ramazani, A. (2018). Synthesis and in vitro evaluation of thermosensitive hydrogel scaffolds based on (PNIPAAm-PCL-PEG-PCL-PNIPAAm)/Gelatin and (PCL-PEG-PCL)/Gelatin for use in cartilage tissue engineering. *Journal of Biomaterials Science. Polymer Edition*, *29*(10), 1185-1206. http://dx.doi.org/10.1080/09205063.2018.1447627. PMid:29490569.
43. Zhu, Z., Xiong, C., Zhang, L., & Deng, X. (1997). Synthesis and characterization of poly (ε -caprolactone) - Poly (ethylene glycol) Block Copolymer. *Journal of Polymer Science. Part A, Polymer Chemistry*, *35*(4), 709-714. http://dx.doi.org/10.1002/(SICI)1099-0518(199703)35:4<709::AID-POLA14>3.0.CO;2-R.

Received: Aug. 21, 2018
Revised: Apr. 16, 2019
Accepted: Apr. 24, 2019

Supplementary Material

Supplementary material accompanies this paper:

Figure S1. Sample amplified region of 1H-NMR spectrum of Reaction A.
Figure S2. Sample amplified region of 1H-NMR spectrum of Reaction B.
Figure S3. Sample amplified region of 1H-NMR spectrum of Reaction C.
Figure S4. Sample amplified region of 1H-NMR spectrum of Reaction D.
Figure S5. Standard polystyrene chromatograms.
Figure S6. GPC standard curve for molecular weight.
Figure S7. Sample FTIR spectrum of PCL.
Figure S8. Sample FTIR spectrum of F127.
Figure S9. Molar mass curve based on FTIR data for reactions with F127.
Figure S10. Molar mass curve based on FTIR data for reactions with PEG.
Figure S11. DSC curve of PCL.
Figure S12. DSC curve of F127.
Figure S13. Sample DSC curve of reaction B.
Figure S14. Sample FTIR spectrum of Reaction C.
Figure S15. Sample FTIR spectrum of Reaction D.
This material is available as part of the online article from http://www.scielo.br/po